Journal of the Physical Society of Japan
Vol. 68, No. 5, May, 1999, pp. 1585-1591

Wavelet Correlation between Electrostatic and Magnetic Plasma Oscillations in the Tokamak TBR

Maria V. A. P. HELLER, Zoezer A. BRASILIO, Iberê L. CALDAS and Raul M. CASTRO

Institute of Physics, University of São Paulo, C.P. 66318, 05315-970 São Paulo, SP, Brazil

(Received September 21, 1998)

Wavelet spectrum and bispectrum techniques were applied to study nonstationary turbulence at the plasma edge of the TBR tokamak. Evidence of nonlinear phase coupling is more significant for magnetic than for electrostatic fluctuations. On a single discharge basis, the data also exhibit intermittent episodes of linear and nonlinear coupling between electrostatic and magnetic field oscillations. Furthermore, application of resonant perturbing magnetic fields reduces the amplitude of low frequency fluctuations and shift the frequency range of the maximum quadratic intermittent coupling to larger scales. These alterations, observed not only for magnetic but also for electrostatic oscillations, support the possibility of roughly altering electrostatic oscillations, therefore transport, through controlling oscillating magnetic fields.

KEYWORDS: turbulence, tokamak, wavelet

§1. Introduction

Application of tokamak as an efficient fusion device depends on a better understanding of the phenomenon of turbulence that dominates the plasma edge and causes strong transport and poor energy confinement.[1,2] Despite the amount of experimental data[1,2] and some theoretical investigations[3-7] the driving sources of plasma edge turbulence are only partially identified. Particularly, the measured broadband spectra of this turbulence are not well reproduced by present models.[8] Less known are higher order moments associated to coupling coefficients of the main frequency components involved in the energy cascading process characteristic of turbulence.[9]

One peculiar coupling theoretically discussed in the literature is that between magnetic and electrostatic turbulent oscillations. It has been predicted that this coupling could affect the transport under some plasma conditions.[10,11] On the other hand, even so experimental measurements in magnetically confined plasmas show that transport is dominated by electrostatic turbulence,[1,2] in some devices as the reverse field pinch magnetic turbulence also contributes to transport.[12-14] Moreover, there are other evidences of correlation between these oscillations, as for example modulation of electrostatic turbulence by dominant magnetohydrodynamic modes.[15]

There is no general understanding on the influence of magnetic oscillations on electrostatic fluctuations observed in magnetically confined plasmas. Consequently, it is important to look for experimental evidences of this coupling and to compare these results with theoretical predictions that describe the possible influence of magnetic turbulence on the transport.

Thus, correlation between electrostatic and magnetic edge fluctuations was studied in the Brazilian tokamak TBR considering the peculiar feature of this device that is the partial superposition of these fluctuations frequency spectra.[16]

Initially, we applied traditional Fourier analysis to quantify correlation between these two nonstationary fluctuating quantities.[16] This technique involves long time averages of data in which stationary fluctuations can be expressed as a superposition of sinusoidal functions. Our previous results detected correlations essentially between temperature and magnetic poloidal field fluctuations. We found no clear evidence of correlations between other electrostatic fluctuations and poloidal magnetic field fluctuations. However, with this analysis we could not identify intermittent behavior of the oscillations. After that, to overcome this problem, we applied wavelet analysis to our turbulent data and determined local information about intermittent correlation at a particular frequency band and temporal location in the time-scale plane. So, in this paper we present new features concerning correlation and coupling that have not been previously observed.

Furthermore, as turbulence arises typically in nonlinear systems,[17] we also used wavelet analysis to apply bispectra as a method for the detection of intermittent quadratic phase coupling on the studied oscillations.[18-20]

For these oscillations, we also found the response of linear and nonlinear coupling to applied magnetic perturbations created by resonant helical winding placed around the torus. Thus, we studied how these couplings changed with the fluctuating magnetic field spectra.

The outline of this article is as follows; §2 presents a general introduction to the linear and bicoherence spectral wavelet analysis that is appropriate for the treatment of our nonstationary signals. Section 3 gives the description of the experimental set-up. Section 4 describes the wavelet spectral characteristics of the measured magnetic and electrostatic fluctuation fields, with or without the external resonant perturbation. Section 5 discusses the coupling between electrostatic and magnetic oscillations,

and §6 presents the conclusions of this work.

§2. Spectral and Bispectral Wavelet Analysis

A basic aspect of turbulent behavior of plasma edge parameters is intermittency.[8] However, as the amplitude and spectral characteristics of fluctuating quantities vary on a short time scale, to study intermittency we need an analysis technique not supported by an accumulation of data over time scales larger than the intermittent characteristic time scale. In other words, we need a technique that does not averages the dynamics and shadows relevant information. To overcome this problem, we used wavelet analysis,[21] for which time resolution varies with frequency. Signals are decomposed into oscillations that die out in time, and more rapidly so the higher their frequencies, what seems a picture more convenient for turbulence than the usually assumed Fourier stationary oscillations.

The wavelet method is based on a wavelet function set that changes its size and position by dilation and shifting. The wavelet transform decomposes the signal using a wavelet basis of functions localized both in time and frequency. A good frequency resolution needs a large sampling window, which results in a poor time resolution; conversely, a good time resolution implies short windows, which results in a poor frequency resolution. This multiresolution feature is useful for analyzing nonstationary fluctuations.

We used the continuous wavelet transform based on the wavelet,[18]

$$\psi_a(t) = a^{-1/2} \exp[\mathrm{i}2\pi t/a - (t/a)^2/2], \qquad (1)$$

where a is the scaling parameter, for which we assign the frequency $f = 1/a$. The frequency resolution of these wavelets is $\Delta f = f/4$ and the time resolution is $\Delta t = 2a$. For a signal $x(t)$ the wavelet transform with respect to the chosen wavelet is defined by:[21]

$$W(\boldsymbol{a}, \tau) = \int x(t)\psi_a(t-\tau)\mathrm{d}t, \qquad (2)$$

where τ is a time shift parameter. The wavelet transform at any given parameter a can be interpreted as a filtered version of $x(t)$ bandpassed by the filter ψ_a.

Similarly to Fourier spectral analysis, we defined the cross-power spectrum for two time series $x(t)$ and $y(t)$. Consequently, the phase, θ_{yx}, and the coherence, γ_{yx}, spectra are defined in the usual way, using wavelet transform instead of Fourier transform.

The wavelet method can be applied to obtain the wavenumber-frequency spectrum, $S(k, f)$,[22] and from this the $S(f)$ and $S(k)$ spectra. From $S(k, f)$ we also determine the power weighted average values of poloidal wave-vector, k, and the phase velocity $v_{\mathrm{ph}} = 2\pi f/k$.

Once turbulence generally arises in nonlinear systems, we need an analysis method capable to calculate this nonlinearity. Wavelet and bispectral analysis can be combined to obtain phase coupling between wavelet components of different scale lengths.[18-20, 23] Wavelet-bispectrum measures the amount of phase coupling that occurs between wavelet components of scale lengths a_1, a_2, and a, such that the sum rule $1/a = 1/a_1 + 1/a_2$ is satisfied. Since scale lengths may be interpreted as inverse of frequencies we can use $f = f_1 + f_2$. The wavelet bispectrum is given by:

$$B(f_1, f_2) = \int_T W_x^*(f, \tau) W_x(f_1, \tau) W_x(f_2, \tau)\mathrm{d}\tau, \qquad (3)$$

where the integral is taken on a finite interval T as in the linear-wavelet spectrum. The triple product of this equation depends of the wavelet transform signal. In the case that phases are coupled the product will not change sign randomly and the bispectrum will have a nonzero value.

In this work we calculated the normalized wavelet bicoherence, $0 < b^w(f_1, f_2) < 1$, plotted over the corresponding frequency space (f_1, f_2). The interaction region includes both sum and difference $(f_1 \pm f_2)$ interactions.

To compare cases computed under the same numerical conditions it is useful to define the summed-bicoherence as:

$$[b^w(f)]^2 = 1/s(f) \sum [b^w(f_1, f_2)]^2, \qquad (4)$$

where the sum is taken over all f_1 and f_2 such that the summation rule is satisfied and $s(f)$ is the number of terms of each f. Summing in f, we can obtain also the total-bicoherence. As wavelet analysis can be calculated for short data sequences, the alterations of total bicoherence values during a discharge time can identify intermittent behavior.

The wavelet crossbispectrum $B_{yx}(f_1, f_2)$ measures the amount of phase coupling in the interval T that occurs between wavelet components of frequencies f_1 and f_2 of the signal $x(t)$ and the wavelet component f of the signal $y(t)$ such that the sum rule $f = f_1 + f_2$ is satisfied. Thus, we calculated the wavelet crossbicoherence from electrostatic and magnetic fluctuating fields measured at two nearby points to obtain the amount of quadratic coupling between these oscillations.

§3. Experimental Set-Up

The experiment was accomplished in the Ohmically heated TBR tokamak ($R_0 = 0.30\,\mathrm{m}$, minor radius $a = 0.08\,\mathrm{m}$, toroidal magnetic field $B_\phi = 0.4\,\mathrm{T}$, plasma current $I_\mathrm{p} = 10\,\mathrm{kA}$, chord average density $n_0 = 7 \times 10^{18}\,\mathrm{m}^{-3}$, safety factor at the limiter $q(a) = 4.5$). We constructed and installed at TBR a complex system of probes to measure simultaneously the electrostatic and magnetic fluctuations and some plasma parameters. More details of the experiment can be found elsewhere.[24, 25] This probe system allows the measurement of the following quantities: mean electron temperature, ion saturation current, floating potential and their corresponding fluctuations, and two points estimates of poloidal wave numbers. A pair of magnetic coils mounted in the same system measures the poloidal component of magnetic field fluctuations. The probe was mounted on a single movable shaft allowing radial profile measurements in separate discharges. The signals were digitized at a sampling frequency of 1 MHz. In this work we show spectra from electrostatic fluctuations measured at $r/a = 0.85$ and magnetic fluctuations at $r/a = 1.07$.

The magnetic field perturbation was created by an electric current ($I_h = 280$ A) through a resonant helical winding (RHW) externally placed around the torus.[26] The RHW coils produce a perturbation field with dominant helicity $m = 4/n = 1$, and an average radial amplitude $\langle |b_r(a)/B_\phi| \rangle \approx 0.4\%$ at the limiter radius. Such perturbation was resonant with the plasma region with safety factor $q = 4$. In this experiment, the application of the external field perturbation does not alter the global equilibrium discharge conditions but create a perturbed resonant field line configuration similar to those obtained with ergodic divertors in TEXT[27] and TORE SUPRA tokamaks.[28]

§4. Wavelet Spectral Characteristics of Field Fluctuations

Electrostatic and magnetic probe measurements of electrostatic and magnetic fluctuations on the plasma edge have been performed on several tokamaks. Despite the differences among tokamaks, some turbulence properties are commonly observed in their plasma edge.[1,2]

Electrostatic fluctuations are mainly transverse to the magnetic toroidal field with the power concentrated on a broad range frequency decreasing to high frequencies. Generally, fluctuation levels are of the order of 10–20%. Phase velocities are comparable to drift velocities. Mirnov or poloidal magnetic oscillations have much lower amplitudes, high phase velocities, and lower frequencies in comparison with the electrostatic fluctuations. Magnetic spectra have both resonances and turbulent components.

Different to most tokamaks, the main frequencies of the TBR electrostatic fluctuation spectra are in the same frequency region than Mirnov frequencies.[16] This peculiarity is a consequence of the plasma radius and the magnetic toroidal field values and fits known scaling laws.[1,2,26] So, this peculiar superposition of the observed magnetic and electrostatic spectra allows us to study linear and quadratic correlations between components of electrostatic and magnetic spectra.

We have analyzed the ion saturation current ($\tilde{I}_{si}$), potential ($\tilde{\varphi}$), temperature ($\tilde{T}_e$), and poloidal magnetic field ($\tilde{B}_\theta$) fluctuations at edge and scrape-off-layer (SOL) of TBR tokamak. To examine the time behavior of the fluctuations we split the data into three consecutive segments of 1024 data points, applying the wavelet analysis for each segment. All the measured fluctuations exhibit broadband wavelet spectra. Figure 1 shows the superposition of the spectra of the electrostatic and magnetic fluctuations measured at $r/a = 0.85$ and $r/a = 1.07$, respectively, for an interval of 1.02 ms. Similar spectra are observed for all time and radial positions. The referred superposition is more pronounced between potential, temperature, and poloidal magnetic field fluctuations. Predominant magnetic fluctuations occurred in a broadband frequency range at $f \approx 50$ kHz with amplitudes $B_\theta^{rms}/B_\theta(a) \approx 1.2 \times 10^{-3}$, where B_θ^{rms} is the root mean square of the poloidal magnetic field fluctuations.

The perturbing external resonant field modifies all the measured fluctuations. Figure 2 shows fluctuation spectra obtained with or without the perturbing fields; we

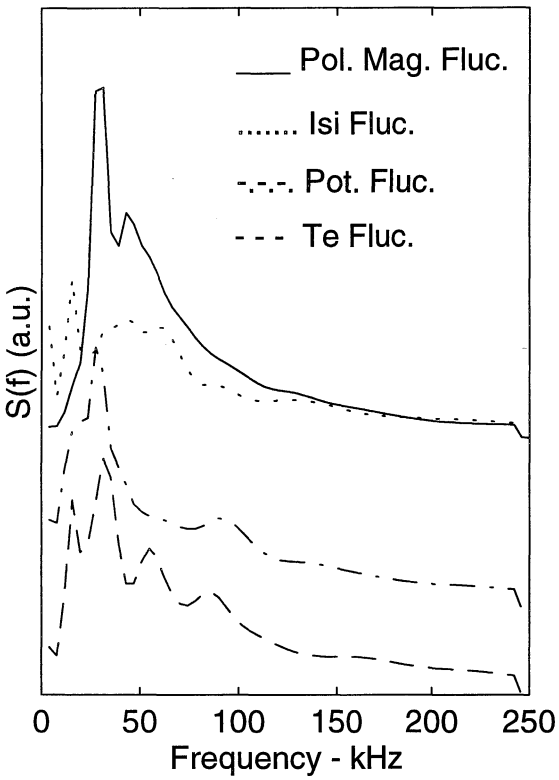

Fig. 1. Spectra superposition of poloidal magnetic field fluctuations (——) at $r/a = 1.07$, ion saturation fluctuations (·····), potential fluctuations (–·–·–), and temperature fluctuations (– – – –) at $r/a = 0.85$. For a choosen time interval of 1.02 ms of a discharge.

can observe a substantial decreasing of spectral densities and a slow down of frequencies for the magnetic spectrum. This perturbation creates both a primary magnetic island on the resonant surfaces with $q = 4$ and chaotic regions near this surface. Chaos, due to the interaction of the primary and secondary magnetic islands near the resonant surface, destroyed the magnetic surfaces creating a chaotic layer at the plasma edge. The observed spectral alterations are attributed to the different plasma connections to the walls, along the chaotic field lines, resulting in a larger area reached by the plasma and a reduction of plasma density. In addition, the plasma potential may self-organize because of the ambipolarity to the wall since the field lines in the chaotic layer reaches the wall.[29] Thus, this density reduction changed the magnetohydrodynamic equilibrium profiles altering the turbulence spectral characteristics.

As our system permits simultaneous two-point measurements of electrostatic and magnetic fluctuations we calculated from the wavenumber-frequency spectrum, $S(k, f)$, the statistical dispersion relation, $k(f)$, coherency spectrum, $\gamma_{yx}(f)$, and phase velocity, v_{ph}. As in other tokamaks,[1,2] the dispersion relations were linear for electrostatic and for poloidal magnetic fluctuations, and the spectral width $\sigma_k/k > 1$. However, since we are using wavelet analysis, in this work we can observe that the values of these parameters varied during the discharge. As usual, propagation velocities for magnetic fluctuations were in the electron drift direction, while the electrostatic fluctuation velocities were in the ion dia-

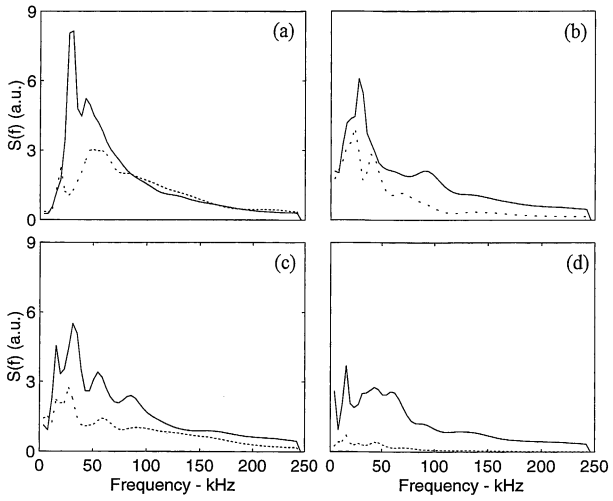

Fig. 2. Spectra of poloidal magnetic field fluctuations with (·····) or without (——) external perturbing fields (a). The same for potential fluctuations (b), temperature fluctuations (c), and ion saturation current fluctuations (d).

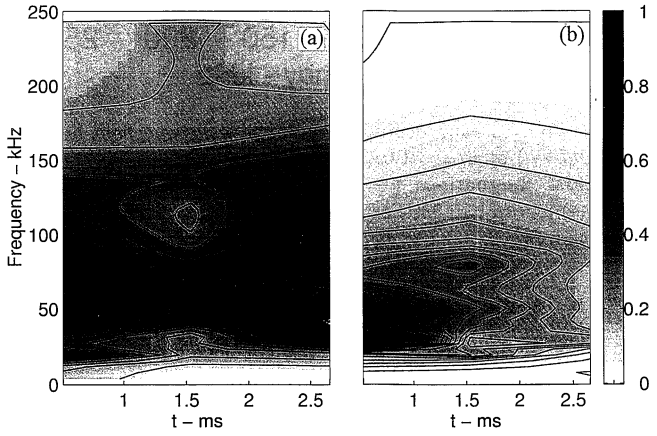

Fig. 3. Time-scale $S(f)$ wavelet spectrum for poloidal magnetic field fluctuations with (a) or without external magnetic field perturbation (b).

magnetic drift direction. As in other tokamaks,[30] the magnetic phase velocities were much higher than those of electrostatic fluctuations. The external field perturbations attenuated the high k waves, specially for magnetic fluctuations, affecting the phase velocities.

Figure 3 shows the time-scale wavelet spectrum for poloidal magnetic field fluctuations with 3(a) or without 3(b) the external magnetic field perturbation, during the analyzed discharge. The spectra show time intermittency that was not previously identified using Fourier analysis with time series for seven consecutive shots.[16] The same behavior was obtained analyzing two-point ion saturation and floating potential probes.

Comparisons of our results with estimations of fluctuation levels and wave vectors from drift waves and rippling mode models[3-5] show that our values are compatible to rippling mode model.

§5. Linear and Quadratic Coupling between Electrostatic and Magnetic Fields

We used wavelet coherence and bicoherence spectra[18-20,31-33] to identify evidences of linear and nonlinear (quadratic) interactions between the measured electrostatic and magnetic fluctuations in the time-scale domain.

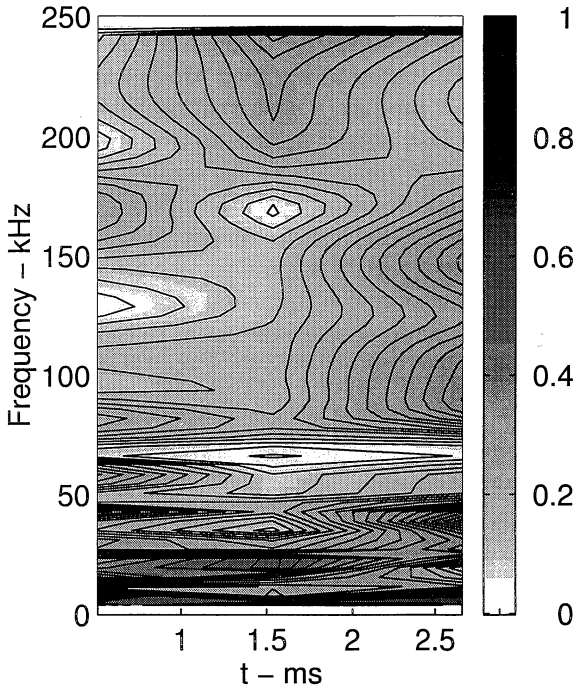

Fig. 4. Time resolved wavelet coherence between floating potential and poloidal magnetic field fluctuations without external magnetic perturbation.

So, electrostatic and magnetic fluctuations were simultaneously measured with probes separated by 1.8×10^{-2} m in the radial direction. Estimated correlations between these fluctuations are reliable, as they extend beyond the correlation length of electrostatic (0.6×10^{-2} m) and magnetic (3.0×10^{-2} m) fluctuations.

Figure 4 shows the time resolved wavelet coherence between floating potential and poloidal magnetic field fluctuations with external magnetic perturbations. Time resolution is 1 ms and the noise level, estimated according reference,[19] is $\approx$0.10 for low frequency components. In this graph the contour lines connect areas of equal coherence. The coherence is highly intermittent and, for low frequencies, the spectral regions of high-power density, high values are achieved, up to 0.8. Moreover, the highest coherences occur in the range of frequencies that account for most of the transport.[16] Similar results were obtained for coherence between poloidal magnetic field and ion saturation current or electron temperature fluctuations. In contrast, previous conclusions obtained with Fourier-based analysis (applied on seven consecutive discharges) gave relevance only to coherence between temperature and magnetic field fluctuations. Data without the external perturbation showed a similar behavior. Therefore, the significative linear coherence between magnetic and electrostatic fields shows that a fraction of magnetic fluctuation power may be due to local electrostatic fluctuations. Moreover, in this work wavelet analysis permits to extract intermittent features, not quite evident with Fourier analysis, changing our previous con-

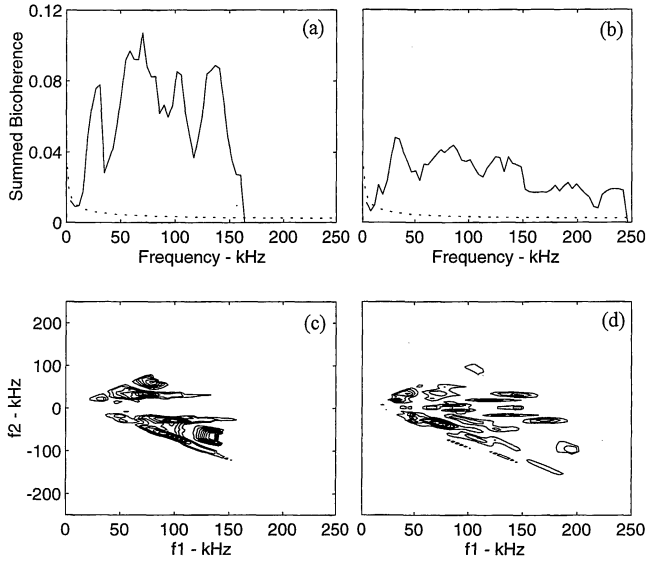

Fig. 5. Summed autobicoherence for poloidal magnetic field fluctuations without external magnetic perturbation for a selected time interval of 1.02 ms (a), contour plot of autobicoherence of the same fluctuations (c). Summed autobicoherence for potential field fluctuations (b) and contour plot of autobicoherence of the same fluctuations (d). Maximum autobicoherence values are 0.26 (a) and 0.20 (b); statistical error for summed autobicoherence indicated by dashed lines.

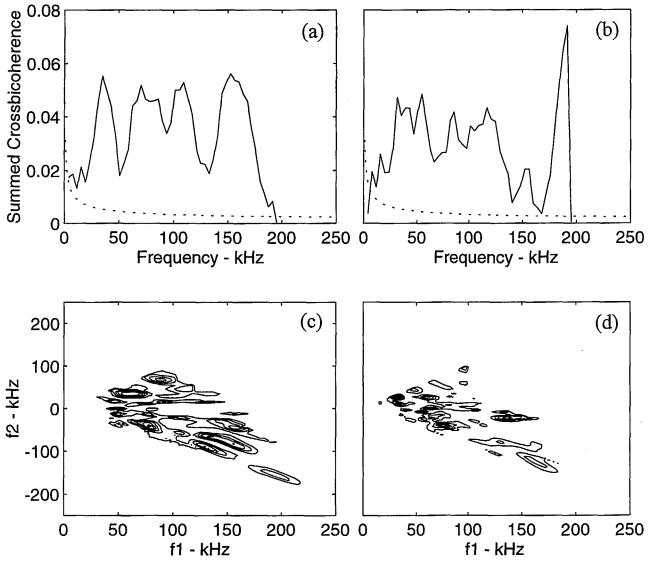

Fig. 6. Summed crossbicoherence for poloidal magnetic field and temperature fluctuations (a), contour plot of crossbicoherence of the same fluctuations (c). Summed crossbicoherence between poloidal magnetic field and potential field fluctuations (b) and contour plot of crossbicoherence of the same fluctuations (d). Maximum crossbicoherence values are 0.16 (a) and 0.21(b); maximum statistical error for summed crossbicoherence is indicated by dashed lines.

clusions.[16]

To examine how the quadratic interactions are spread in frequencies, we estimated the squared wavelet bicoherence, $b^w(f_1, f_2)$, and the summed wavelet bicoherence, $b^w(f)$, on a frequency grid with 256 points from 0 to 1 MHz, for selected data from successive intervals of 1.02 ms during the plasma discharge. The results, for the first interval, without external field perturbations, are presented in Fig. 5. In Figs. 5(a) and 5(c) we have the summed autobicoherence and the contour plot of autobicoherence for poloidal magnetic field fluctuations. Figures 5(b) and 5(d) show the same for potential fluctuations. As the numerical values of summed bicoherence depend on the chosen calculation grid, we compared cases computed under the same numerical conditions. Nonlinear interactions are more significative and better defined for magnetic than for potential fluctuations. All the summed bicoherence values are significantly above the statistical uncertainty.[19] Similar autobicoherence spectra are observed for ion saturation and temperature fluctuations.

The crossbicoherence values calculated between the poloidal magnetic field and the electrostatic fluctuations show similar values but a strong intermittency through the discharge. Figures 6(a) and 6(c) show the summed crossbicoherence between the poloidal magnetic fluctuations and temperature fluctuations for an interval of 1.02 ms, and the contour plot of the crossbicoherence between the same fluctuations. Figures 6(b) and 6(d) show the same quantities for the poloidal magnetic field and the potential fluctuations. Dashed lines show the statistical uncertainties. The values of the quadratic coupling are high compared with the statistical error. In the two cases couplings are in low and medium frequency regions

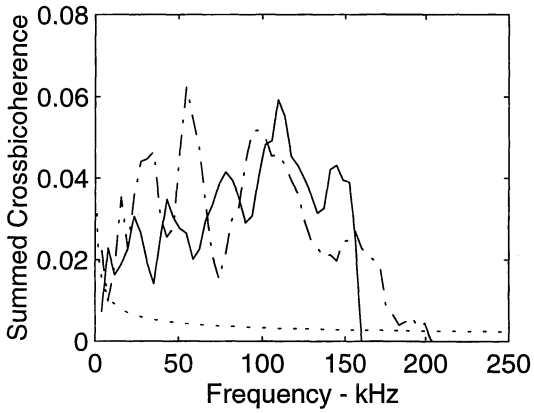

Fig. 7. Summed crossbicoherence between poloidal magnetic field and ion saturation current fluctuations with (–·–·–·) or without (——) the resonant perturbing field. Dashed line is the statistical error.

and in both sum and difference frequency regions.

Figure 7 shows the summed crossbicoherence between the poloidal magnetic field and the ion saturation fluctuations with or without the external perturbing magnetic field. The effect of this perturbation on the fluctuations is observed in this figure: enhancement of low frequency components and spread to higher frequency. However, the intermittency is always present during the discharge.

A summary of the quadratic coupling behavior is observed in Table I that shows the total autobicoherence and total crossbicoherence for the measured fluctuations for the first chosen interval of the discharge. The external magnetic perturbation clearly has distinct reverse effects on the magnetic poloidal field and potential fluctuations, increasing the total autobicoherence of the first fluctuation and decreasing it for the second fluctuation.

Table I. (a) shows the total autobicoherence values of the measured fluctuations for a selected time interval of a discharge without or with the external perturbation fields (RHW). (b) shows the total crossbicoherence between poloidal magnetic field and the measured fluctuations without or with the perturbing fields (RHW). All the table values are multiplied by 1×10^{-2}. Maximum statistical error is $\approx 1 \times 10^{-2}$.

(a) Total autobicoherence.

$\tilde{B}_\theta$	$\tilde{B}_\theta$ RHW	$\tilde{\varphi}$	$\tilde{\varphi}$ RHW	$\tilde{I}_{si}$	$\tilde{I}_{si}$ RHW	$\tilde{T}_e$	$\tilde{T}_e$ RHW
8	12	7	4	3	4	3	3

(b) Total crossbicoherence.

$\tilde{B}_\theta\tilde{B}_\theta$	$\tilde{B}_\theta\tilde{B}_\theta$ RHW	$\tilde{\varphi}\tilde{B}_\theta$	$\tilde{\varphi}\tilde{B}_\theta$ RHW	$\tilde{I}_{si}\tilde{B}_\theta$	$\tilde{I}_{si}\tilde{B}_\theta$ RHW	$\tilde{T}_e\tilde{B}_\theta$	$\tilde{T}_e\tilde{B}_\theta$ RHW
10	4	4	3	4	3	4	3

On the other hand, no evident alteration was induced by the external perturbation on the total autobicoherence of ion saturation and temperature fluctuations. In the total crossbicoherence between electrostatic and magnetic fluctuations we verified almost no effect of the external perturbations. Similar observations were obtained on the others intervals of the discharge.

§6. Conclusions

To investigate linear and quadratic correlations between electrostatic and magnetic fluctuations we analyzed data obtained from a complex probe system at TBR tokamak plasma edge.

We used a wavelet approach to analyze single time series and two time series in which the fluctuating quantities are nonstationary. Relative short data sequences are sufficient to perform the analysis, in contrast to Fourier technique that needs long time series to obtain sufficient frequency resolution and statistics. Estimates of error levels of wavelet calculations provide a criterion for the reliability of results. Therefore, we conclude that wavelet analysis is convenient to study intermittent interactions of these nonstationary signals, removing the assumption that turbulence signals consist of modes that are constant in time. Even so, wavelet analysis preserves the physical intuition associated to mode description by assigning a frequency to each wavelet scale. Our previous results obtained with Fourier analysis relayed on the accumulation of data over time scales larger than the characteristic time scale of the measured plasma turbulence, averaging out much of the dynamics and destroying relevant information about coupling.[16]

The measured turbulence spectra are similar to those obtained in other tokamaks.[1,2] Thus, electrostatic fluctuations are mainly transverse to the magnetic toroidal field with the power concentrated on a broad range frequency decreasing to high frequencies, and fluctuation levels are of the order of 10–20%. Moreover, electrostatic phase velocities are comparable to drift velocities. Poloidal magnetic oscillations have much lowers amplitudes, high phase velocities, and lower frequencies in comparison with the electrostatic fluctuations. Magnetic spectra have both resonances and turbulent components. Different to most tokamaks,[1,2] as a consequence of TBR plasma radius and magnetic toroidal field values,[1,26] the main frequencies of electrostatic fluctuation spectra are in the same frequency region than Mirnov frequencies.[16]

In the present wavelet analysis we also showed the evolution of the investigated spectra, identifying intermittent couplings. Indeed, linear and quadratic interactions varied during discharge, showing that the phase coupling process is intermittent. On the other hand, both analyses show that nonlinear coupling is more significative for poloidal magnetic field than for electrostatic field.

Few results have been reported about applications of bispectral analysis on tokamak turbulence. One example is a coherent peak in the electrostatic plasma edge turbulence observed in the tokamak TEXT, by applying Fourier bispectral analyses to data probes.[34] However, we do not observe only one isolated coherent peak in our bicoherence, but some peaks spread in the examined frequency range. Another example is the Fourier bispectral analysis applied to analyze the turbulence development on the toroidal device Thorello for plasma confined in a low density and low magnetic field toroidal device.[35] A wavelet bispectral analysis was applied to investigate L/H mode transitions on the Continous Current Tokamak.[19] This work shows higher bicoherences for H mode and intermittency similar to our experiment.

With the Fourier analysis we detected correlations essentially between magnetic poloidal field and temperature fluctuations.[16] On the other hand, the wavelet analysis showed significative correlations between this magnetic field and other electrostatic fluctuations. These results confirm our previous results and reinforce the possibility that these fluctuations have a partial common driving process as discussed in ref. 36. These correlations are expected if magnetic fluctuations in the plasma edge are due to the currents driven by electrostatic turbulence.[30]

Moreover, with this wavelet analysis we also found higher quadratic coupling, between the electrostatic and poloidal magnetic fluctuations, than that previously obtained with Fourier analysis.[16] This coupling could be important for energy transfer between electrostatic and magnetic frequency components as predicted in some models.[11] Further complete results from bicoherence between magnetic and electrostatic fluctuations are not yet available in the literature.

Resonances created by external magnetic fields reduce the amplitude of fluctuations and shift the frequency range of the maximum quadratic coupling to larger scales (lower frequency components). The effect of this perturbation is to reduce slightly but intermittently the quadratic coupling. Alterations on spectral distributions due to external field perturbations suggest a global decrease of turbulence level. This resonant perturbation creates magnetic islands and a chaotic layer near the plasma edge. This modification of magnetic structure should alter the fluctuation spectra due to the different plasma connections to the walls along the chaotic field lines. As it has been suggested,[29] the plasma potential may self-organize because of this ambipolarity to the wall. Thus, this change on the magnetohydrodynamic

equilibrium profiles could alter the turbulence spectral characteristics.

So, in this work we confirm the reliability of wavelet transform to analyze plasma edge turbulence. Thus, applications of this technique could be further developed to study other turbulence features as formation and lifetime of coherent structures, and direction of their carried energy flow.[17] However, for these studies we need other kind of diagnostics or two-dimensional long rows of electrostatic probes.

Finally, our results of fluctuation levels and wave vectors are compatible with values estimated from rippling mode model.[3-5] However, a theoretical description of our observations, concerning the intermittent coupling between magnetic and electrostatic fluctuations, has yet to be developed by applying basic plasma turbulence models.[6-8, 11]

Acknowledgements

This work was partially supported by the Brazilian Agencies FAPESP and CNPq.

1) A. J. Wootton, B. A. Carreras, H. Matsumoto, K. McGguire, W. A. Peebles, Ch. P. Ritz, P. W. Terry and S. J. Zweben: Phys. Fluids **2** (1990) 2879.
2) F. Wagner and V. Stroh: Plasma Phys. Control. Fusion **35** (1993) 1321.
3) P. W. Terry and P. H. Diamond: Phys. Fluids **28** (1985) 1419.
4) L. Garcia, P. H. Diamond, B. A. Carreras and J. D. Callen: Phys. Fluids **28** (1985) 2147.
5) T. S. Hahm, P. H. Diamond, P. W. Terry, L. Garcia and B. A. Carreras: Phys. Fluids **30** (1987) 1452.
6) B. D. Scott: Phys. Rev. Lett. **65** (1990) 3289; Phys. Fluids B **4** (1992) 2468.
7) S. J. Camargo and H. Tasso: Phys. Fluids B **4** (1992) 1199.
8) B. D. Scott: Contrib. Plasma Phys. **38** (1998) 171.
9) D. Biskamp: Phys. Rev. E **50** (1994) 2702.
10) D. Biskamp: *Nonlinear Magnetohydrodynamic* (Cambridge University Press, Cambridge, 1993).
11) S. J. Camargo, B. D. Scott and D. Biskamp: Phys. Plasmas **3** (1996) 3912.
12) G. Li, J. R. Drake, H. Bergsaker, J. H. Brzozowski, G. Hellblom, S. Mazur, A. Moller and P. Nordlund: Phys. Plasmas **2** (1995) 2615.
13) P. R. Brunsell, Y. Mayima, Y. Yagi, Y. Hirano and T. Shimada: Phys. Plasmas **1** (1994) 2297.
14) H. Tan and S. C. Prager: Phys. Fluids **28** (1995) 1419.
15) H. Lin: Ph. D. Thesis, University of Texas, Report FRCR#401, Fusion Research Center, Austin, TX, 1991.
16) M. V. A. P. Heller, R. M. Castro, I. L. Caldas, Z. A. Brasilio, R. P. da Silva and I. C. Nascimento: J. Phys. Soc. Jpn. **66** (1997) 3453.
17) S. Kida and K. Ohkitani: Phys. Fluids A **4** (1992) 1018.
18) B. Ph. van Milligen, E. Sánchez, T. Estrada, C. Hidalgo, B. Brañas, B. Carreras and L. Garcia: Phys. Plasma **2** (1995) 3017.
19) B. Ph. van Milligen, C. Hidalgo, E. Sánchez, M. A. Pedrosa, R. Balbín, I. García-Cortés and G. R. Tynan: Rev. Sci. Instrum. **68** (1997) 967.
20) R. Jha, S. K. Mattoo and Y. C. Saxena: Phys. Plasmas **4** (1997) 2982.
21) Chui: *An Introduction to Wavelets* (Academic, New York, 1992).
22) T. Levinson, J. M. Beall, E. J. Powers and R. D. Bengtson: Nucl. Fusion **24** (1984) 527.
23) R. Jha and Y. C. Saxena: Phys. Plasmas **3** (1996) 2979.
24) R. M. Castro, M. V. A. P. Heller, R. P. da Silva, I. L. Caldas, F. T. Degasperi and I. C. Nascimento: Rev. Sci. Instrum. **68** (1997) 4418.
25) R. M. Castro, M. V. A. P. Heller, I. L. Caldas, Z. A. Brasilio, R. P. da Silva and I. C. Nascimento: Phys. Plasmas **3** (1996) 971; *ibid.* **4** (1997) 329.
26) M. V. A. P. Heller, R. M. Castro, Z. A. Brasilio, I. L. Caldas and R. P. da Silva: Nucl. Fusion **35** (1995) 59.
27) S. C. McCool, A. J. Wootton, A. Y. Aydemir, R. D. Bengtson and J. A. Oedo: Nucl. Fusion **29** (1989) 547.
28) A. Grosman, P. Gendrigh, C. Demichelis, P. Mourier-garbet, J. C. Vallet, H. Capes, M. Chantelier, T. E. Evans, A. Geraud, M. Góniche, C. Grisolia, D. Guilhem, G. Harris, W. Hess, F. Nguyen, L. Poutchy and A. Samain: J. Nucl. Mater. **196** (1992) 59.
29) S. Takamura, N. Ohnishi, H. Yamada and T. Okuda: Phys. Fluids **30** (1987) 144.
30) G. Vayakis: Nucl. Fusion **33** (1993) 547.
31) Ch. P. Ritz and E. J. Powers: Physica 1D **20** (1986) 320.
32) Ch. P. Ritz, E. J. Powers and R. D. Bengston: Phys. Fluids B **1** (1989) 153.
33) S. Santoso, E. J. Powers, R. D. Bengtson and A. Ouroua: Rev. Sci. Instrum. **68** (1997) 898.
34) H. Y. W. Tsui, K. Rypdal, Ch. P. Ritz and A. J. Wootton: Phys. Rev. Lett. **70** (1993) 2565.
35) C. Riccardi, D. Xuantog, M. Salierno, L. Gamberale and M. Fontanesi: Phys. Plasmas **4** (1997) 3749.
36) Y. J. Kim, K. W. Gentle, Ch. P. Ritz, T. L. Rhodes and R. D. Bengtson: Phys. Fluids B **3** (1991) 674.